DISCRETE ELEMENT METHOD (EDEM) SIMULATION AND PARAMETER OPTIMIZATION: DESIGN AND TESTING OF A LOW-LOSS AND HIGH-EFFICIENCY CORN THRESHING DEVICE

/

离散元法（EDEM）仿真与参数优化： 低损高效玉米脱粒装置的设计与试验

Yaxiu HOU[1)], Shuqi SHANG, Xiang LI, Xiaoning HE, Haifeng ZHENG, Tongtong DONG, Xu LI, Zhixin LIU, Shuai YANG, Dongwei WANG*

[1)] Qingdao Agricultural University, College of Mechanical and Electrical Engineering / China;

Tel: +86-0532-58957391; E-mail: 200701031@qau.edu.cn

DOI: https://doi.org/10.35633/inmateh-71-16

Keywords: *low threshing efficiency, corn threshers, EDEM simulation, optimized design, test*

ABSTRACT

Aiming at the problems of low threshing efficiency and high damage rate of current threshing devices. In this study, the operational form of the threshing drum and the structure of the threshing element were innovated, and a new threshing drum with low damage and high efficiency was designed. Using EDEM software, flexible body modeling of corn kernels, cobs and whole ears was carried out. The dynamic analysis of the corn threshing process was completed and the simulation parameters were further optimized. The optimum operating parameters were analyzed by orthogonal rotational tests and response surface method with a speed of 800 r/min for the threshing drum, a clearance of 10 mm for the concave plate and 30 mm for the threshing drum. The radius of the round head of the threshing element was 5 mm. The height of the threshing element was 60 mm. The final threshing efficiency was 98.78% and the damage rate of threshing was 0.62%. The results show that the new threshing device can meet the requirements of low-loss threshing devices for corn combine harvesters and can provide a theoretical basis for the development of the theory and technical system of corn plot combine harvesters in the future.

摘要

针对现有脱粒装置脱粒效率低、损伤率高的问题。本研究对脱粒滚筒的工作形式和脱粒元件的结构进行了创新，设计出了一种低损伤、高效率的新型脱粒滚筒。利用 EDEM 软件对玉米籽粒粒、玉米芯和玉米果穗进行了柔性体建模。完成了玉米脱粒过程的动态分析，并进一步优化了模拟参数。通过正交旋转试验和响应面法分析了最佳运行参数，脱粒滚筒转速为 800 r/min，凹板间隙为 10 mm，脱粒滚筒间隙为 30 mm，脱粒元件圆头半径为 5 mm。脱粒元件的高度为 60mm。最终脱粒效率为 98.78%，脱粒损伤率为 0.62%。结果表明，新型脱粒装置能满足玉米联合收获机低损脱粒装置的要求，可为今后玉米小区联合收获机理论和技术体系的发展提供理论依据。

INTRODUCTION

As one of the most important food and feed crops in the world, maize has high production potential and economic benefits with edible, forage, and multiple industrial uses (*Yang et al., 2022*). However, there are many deficiencies in China's corn threshing technology, which seriously affect the development of China's corn industry (*Zhou et al., 2022*). Corn threshing is a key link in the corn harvesting process and the core technology of the corn combine. The structural design and threshing effect of the corn threshing device directly determine the operational performance of the corn combine (*Chen, 2022*). In recent years, in order to improve the effect quality of corn threshing equipment, domestic and foreign scholars have carried out systematic research from many aspects. Srison et al. used EDM to simulate the interaction characteristics of corn seeds, properly quantified the qualitative and directional information of particle flow (*Srison et al., 2016*). Pužauskas et al. created a mathematical model using finite element analysis to study the theory of the maize threshing process, and the relationship between the structural form of the threshing device and the rate of particle fragmentation was analyzed (*Pužauskas et al., 2016*). Zhao Wuyun et al. designed and manufactured a spiral plate tooth-type corn thresher, and established a mathematical model through tests to study and analyze the influence of factors on grain crushing rate during the threshing process and their interactions (*Zhao et al., 2012*).

Li Xinping et al. proposed the theory of "circumferential force circle" and designed a corn bionic machine based on the process of discrete corn kernels by chicken beaks (*Li et al., 2007)*. There is a lack of low-damage threshing devices for small-plot corn harvesting with different moisture content corn varieties, and most of the current simulation studies are based on a rigid model of corn, and establishing a flexible body model of corn is rarely applied in simulation analysis (*Zhou et al., 2021*). In order to analyze the damage of maize kernels during threshing, this paper uses the Hertz collision contact theory (*Wang et al., 2022*) as the basis for maize threshing simulation using the flexible body model, designs the structure of the new threshing element and the threshing device, screens the best working parameters using orthogonal tests, and optimizes the parameters by EDEM simulation, and finally determines the best parameters and verifies the validity of this study by comparing the test results before and after optimization (*Tang et al., 2022*). In this way, a more widely adaptable, high self-cleaning and low-damage plot corn harvester threshing device was designed.

MATERIALS AND METHODS

Determination of physical and mechanical properties related to the corn at maturity

In view of the easy damage of maize in the process of threshing, the mechanical characteristics of maize cob are studied, and several varieties are selected as research objects to establish EDEM flexible body simulation models with the mechanical characteristics of maize cob and maize kernel as indicators (*Li et al., 2021*). A further consideration is given to establish a model of the whole corn cob to simulate the threshing damage when the corn kernels are combined with the corn cob, so as to gain a more comprehensive and in-depth understanding of the threshing damage mechanism. In this experiment, corn kernel crushing rate and corn ear threshing rate were selected as test indexes, and the related physical and mechanical characteristics of corn ear and corn kernel were measured (*Zheng et al., 2020*). A simulation analysis model was created using the EDEM software to serve as a parameter basis for the investigation of the mechanical and physical characteristics of the corn cob. Further design of relevant threshing devices for corn varieties with 25%-35% (*Zhang et al., 2021*) moisture content, depending on the moisture content (*Gao et al., 2022*), and the average physical (*Zhang et al., 2015*) and mechanical characteristics, is shown in Table 1.

Table 1

Determination of the physical and mechanical properties of the components of maize

Parameters	Numerical value
Corn Poisson's ratio	0.40
Corn shear modulus	5.357×10^{7}
Corn density	1197 kg/m^3
Corn-corn recovery coefficient	0.70
Corn-corn static friction coefficient	0.30
Corn-corn rolling friction coefficient	0.04
Poisson's ratio of threshing drum	0.28
Threshing drum density	8000 kg/m^3
Shear modulus of threshing drum	2.93e+10
Corn-threshing drum recovery factor	0.70
Coefficient of static friction of corn-threshing drum	0.30
Coefficient of rolling friction of corn-threshing drum	0.04

Threshing drum element

Studies have shown that the adaptability of the plate teeth or finger plate teeth to the unevenly fed crop layer as well as the strong kneading effect of the grid concave plate with the cob and the obvious tapping and loosening effect on the grain-grass mixture facilitate the separation of the corn threshing material (*Hu et al., 2018*). The structural design of the threshing element with trapezoidal round-headed spike teeth in this study is a combination of the plate threshing drum and spike-tooth threshing drum concepts (*Di et al., 2018*), with the height of the trapezoidal spike teeth ensuring threshing efficiency and the rounded corners of the trapezoidal spike teeth reducing the damage rate of threshing, the general structure of which is shown in Fig.1 (*Yan et al., 2020*).

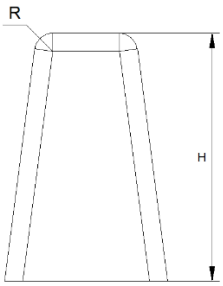

Fig. 1 – Trapezoidal round head nail teeth structure diagram

H: Thresher tooth height; R: The rounded corners of the thresher teeth

Overall structure design

The corn thresher is a longitudinal full-feed device connected with the feed port of the corn combine harvester. The main working parts are lower cover, upper cover plate, combined concave plate, threshing drum, motor and the overall structure is shown in Fig. 2.

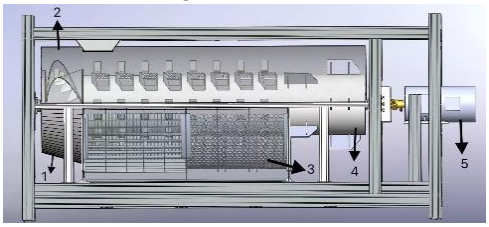

Fig. 2 – Corn threshing device

1. lower cover; 2. upper cover plate; 3. combined concave plate; 4. threshing drum; 5. motor

Compression test

In order to establish a flexible body model for corn, the critical crushing force of corn kernel is firstly determined by mechanical compression test, and then the possible damages during corn kernel threshing are theoretically analyzed based on the collision theory (*China Agricultural Science and Technology Press, 2007*). Since the corn kernel itself is a viscoelastic body, due to the existence of elastic deformation (*Xiao et al., 2021*), the contact centers of the two during the collision will produce displacements close to each other δ_z. The contact between the corn kernel and the threshing element can be regarded as a contact between a sphere and a plane (*Wang et al., 2018*), which leads to the radius of the contact, the distance of the displacement, and the amount of pressure on the contact area between the corn kernel and the threshing element. The results of the corn kernel compression test are shown in Fig. 3.

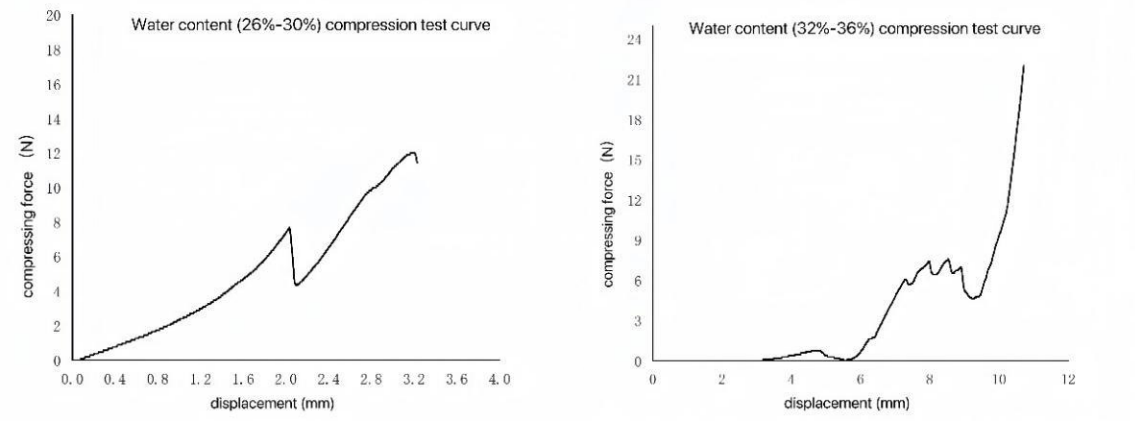

(a) *(b)*

Fig. 3 – The results of the corn kernel compression test

When the contact pressure F_0 between the corn kernels and the threshing element in contact with each other reaches the yield stress limit K of the corn kernels under one-way compression, a point under the surface of the contact area between the two reaches the limit of the elastic state, thus causing the corn kernels to crack or break.

Critical state of corn kernels without plastic deformation is:

$$F_0 = K \tag{1}$$

$$t = t^*, \delta_z = \delta_z^*, F = F^* \tag{2}$$

$$F_0 = \frac{3F}{2\pi ab} = \frac{3F}{2\pi\left(\frac{3p\,R_e}{4E^*}\right)^{\frac{2}{3}}} \tag{3}$$

The maximum contact force between the corn kernels and the threshing element is:

$$F_0^* = \frac{3F^*}{2\pi\left(\frac{3F^*\,R_e}{4E^*}\right)^{\frac{2}{3}}} \tag{4}$$

The maximum critical force of this variety of high moisture content corn kernels is 22.12 N, the maximum displacement is 10.72 mm, that is, when the contact force between the corn kernels and the threshing element reaches the critical force of the broken corn kernels, the relative speed of the two can be found as:

$$v_z = \left\{\frac{2\pi^5 K^5 22.12\,R_e^{\,3}}{60E^{*4}m}\right\}^{\frac{1}{2}} \tag{5}$$

Based on the measured data of the corn compression force, the force and stiffness are calculated by the formula :

$$K = \frac{P}{\delta} \tag{6}$$

Where: K is the stiffness; P is the force, (N); δ is the deformation, (N/m).

The magnitude of the force is taken as 22.12 N and the deformation is taken as 0.0076 N/m to obtain the parameters of the contact between the corn cob and the seed. The normal stiffness per unit area and the shear stiffness per unit area, so as to set the parameters of the Bond model in EDEM.

Bond modeling

Through mechanical compression test and formula calculation, the final Bond model parameters are determined, and the model is established by EDEM. T The model establishment of corn cob, corn kernel and corn ear is shown in Fig. 4, and the modeling parameters are shown in Table 2.

(a) *(b)* *(c)*

Fig. 4 – Bond model:
(a) Corn cob model; (b) Corn kernel model; (c) Corn ear model

Table 2

Parallel Bond Configuration

Parameters	Numerical value
Normal Stiffness per unit area	2.9e+11 N/m^3
Shear Stiffness per unit area	2.9e+11 N/m^3
Critical Normal Stress	3e+10 Pa
Critical Shear Stress	3e+10 Pa
Bonded Disk Radius	1.5 mm

PARAMETER OPTIMIZATION AND EDEM SIMULATION

Parameter optimization

The optimization of the threshing element includes the optimization of the radius of the round head of the threshing element and the height of the threshing element. As shown in Fig. 5 and Fig. 6, the threshing element parameters were imported into EDEM and the results were obtained as shown in Fig. 7, Fig. 8, and Fig. 9.

(a) *(b)* *(c)*

Fig. 5 – Comparison of round head radius design of threshing element:

(a)R=3 mm; (b)R=5 mm; (c)R=8 mm

(a) *(b)* *(c)*

Fig. 6 – Comparison of height design of threshing elements

(a)h_t =50 mm; (b)h_t =60 mm; (c)h_t =70 mm

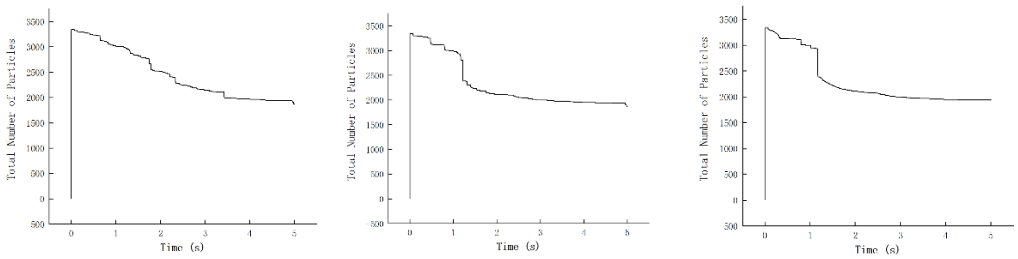

(a) *(b)* *(c)*

Fig. 7 – Contrast results of different heights with rounded corners of 3 mm

(a) R=3 mm, h_t =50 mm; (b) R=3 mm, h_t =60 mm; (c) R=3 mm, h_t =70 mm

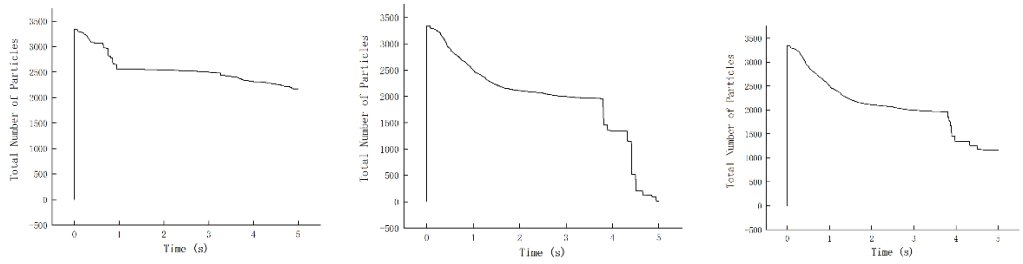

(a) *(b)* *(c)*

Fig. 8 – Contrast results of different heights with rounded corners of 5 mm

(a) R=5 mm, h_t =50 mm; (b) R=5 mm, h_t =60 mm; (c) R=5 mm, h_t =70 mm

(b)

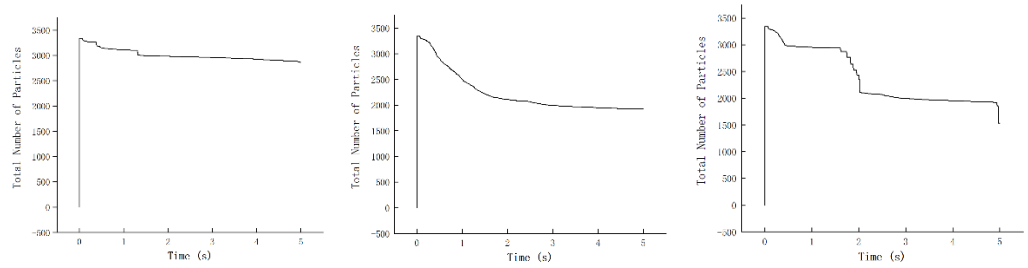

(a) *(b)* *(c)*

Fig. 9 – Contrast results of different heights with rounded corners of 6 mm

(a) R=6 mm, h_t =50 mm;(b) R=6 mm, h_t =60 mm;(c) R=6 mm, h_t =70 mm

The above threshing element is applied to EDEM, and the optimal parameters are finally determined as threshing element height is 60 mm and the radius of the threshing element head is 5 mm.

EDEM simulation

The following data were obtained from the simulation of the threshing drum by EDEM: the threshing rate of 98.78% was calculated using the number of bond breaks and the number of initial bond generation (*Yu et al., 2021*). The loss rate was obtained from the number of bond breaks of corn kernels and the total number of corn kernels (*Li et al., 2022*) to be about 0.32%. In summary, the overall threshing effect was good, but the threshing damage rate was still high, and the threshing rate increased from 96.27% to 98.78% and the threshing damage rate decreased from 2.65% to 0.62% compared with the conventional threshing device (*Qu et al., 2018*), while the designed segmented combined cylindrical threshing concave plate solved the problem of conventional gridded concave plate being blocked by corn cobs, reducing the seed harvesting. The design of the segmented cylindrical threshing concave solved the problem of conventional gridded concaves being clogged by corn bracts and reduced the plugging rate and entrainment losses during harvesting. Threshing simulation is shown in Fig. 10.

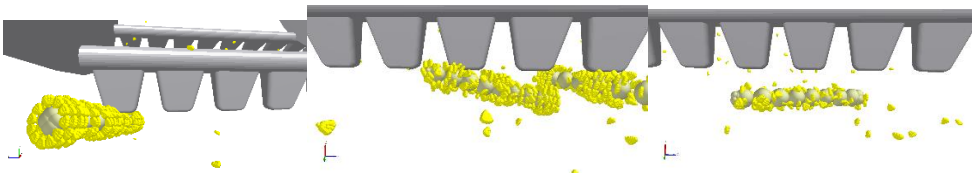

(a) (b) (c)

Fig. 10 – Threshing simulation

(a) Initial; (b) Middle; (c) End

TEST

Corn threshing bench test

The optimized device was machined out of pieces, and a test bed for corn threshing device was constructed for bench testing. The structure of the optimized test bench was shown in Fig. 11. This device adopts the back angle adjustment device and the replaceable threshing nail teeth on the threshing drum, which can carry out different kinds of test verification according to the new threshing nail teeth in the simulation, so that the test process is more convenient and efficient, and the test results can achieve the best effect. The final test result can completely take off the corn kernels and keep the integrity of the corn kernels, the optimal threshing effect of simulation is achieved and the test results are better.

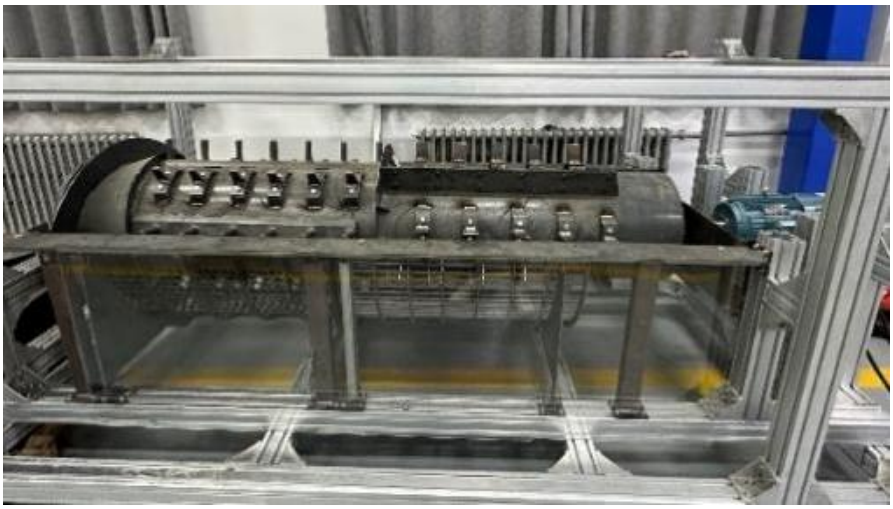

Fig. 11 – Corn threshing device test bench

Based on the experimental experience, the preliminary design of threshing device-related parameters was taken in the range of 9-11 mm for the concave clearance, 25-35 mm for the threshing clearance and 700-900 r/min for the threshing drum speed (*Chen et al., 2022*). The analysis of the orthogonal test was carried out using Design-expert software, and Box-Behnken Design was used for the calculation in order to reduce the number of tests. The factors and levels for orthogonal tests of threshing device parameters are shown in Table 3. The results of the orthogonal test for the parameters of the threshing device are shown in Table 4.

Table 3

Factors and levels for orthogonal tests of threshing device parameters

Level	Concave clearance A (mm)	Threshing clearance B (mm)	Threshing drum speed C (r/min)
-1	9	25	700
0	10	30	800
1	11	35	900

Table 4

Results of orthogonal tests on threshing device parameters

Test number	Concave clearance A (mm)	Threshing clearance B (mm)	Threshing drum speed C（r/min)	Threshing efficiency (%)	Threshing damage rate (%)
1	9	25	800	98.35	0.77
2	11	25	800	98.26	0.84
3	9	35	800	98.21	0.89
4	11	35	800	98.54	0.72
5	9	30	700	97.32	0.88
6	11	30	700	97.23	0.95
7	9	30	900	98.63	0.72
8	11	30	900	98.58	0.84
9	10	25	700	98.38	0.97
10	10	35	700	97.12	0.76
11	10	25	900	98.61	0.93
12	10	35	900	98.57	0.88
13	10	30	800	98.67	0.84
14	10	30	800	97.61	0.95
15	10	30	800	98.57	0.73
16	10	30	800	98.76	0.81
17	10	30	800	98.78	0.62

By comparing the results with the experiments conducted by other researchers, the final results of the threshing device in this paper were obtained to be better than the experimental results of other researchers (*Bi et al., 2015*). According to the results of the orthogonal test, the residuals of the test indexes were drawn (*Li et al., 2015*), and the reliability of the orthogonal test was analyzed. ANOVA was performed on threshing efficiency and threshing damage rate respectively to compare the significance of influencing factors, and the optimal combination of parameters was judged according to the significance effect, and the optimal parameters were finally determined. The ANOVA for threshing efficiency is shown in Table 5. The ANOVA of threshing damage rate is shown in Table 6.

Table 5

ANOVA of threshing efficiency

Source of variance	Mean square	Degrees of freedom	Sum of square	P value
Model	0.6213	9	0.0690	0.0277 < 0.05
A	0.0013	1	0.0013	0.0480 < 0.05
B	0.0032	1	0.0032	0.0457 < 0.05
C	0.2244	1	0.2244	0.0060 < 0.05
AB	0.0441	1	0.0441	0.1289
AC	0.0004	1	0.0004	0.8744
BC	0.0121	1	0.0121	0.3972
A2	0.1203	1	0.1203	0.0250
B2	0.1504	1	0.1504	0.0155
C2	0.0334	1	0.0334	0.1781
Residual	0.1042	7	0.0149	
Lack of fit	0.0423	3	0.0141	0.5108 > 0.1
Pure error	0.0619	4	0.0155	
Sum	0.7255	16		

Note:(P < 0.05 means the item is significant, P > 0.1 means the item is not significant)

Table 6

ANOVA of threshing damage rate

Source of variance	Mean square	Degrees of freedom	Sum of square	P value
Model	0.1206	9	0.0134	0.0005
A	0.0010	1	0.0010	0.0284 < 0.05
B	0.0084	1	0.0084	0.0123 < 0.05
C	0.0465	1	0.0465	0.0001 < 0.001
AB	0.0009	1	0.0009	0.3106
AC	0.0006	1	0.0006	0.3927
BC	0.0049	1	0.0049	0.0381
A2	0.0133	1	0.0133	0.0040
B2	0.0081	1	0.0081	0.0137
C2	0.0313	1	0.0313	0.0004
Residual	0.0053	7	0.0008	
Lack of fit	0.0043	3	0.0014	0.6300 > 0.1
Pure error	0.0010	4	0.0002	-
Sum	0.1259	16		-

Note: (P < 0.05 means the item is significant, P < 0.001 means the item is highly significant, P > 0.1 means the item is not significant)

After analyzing the above two tables, it can be concluded that the effects of concave plate gap and threshing gap of threshing drum on threshing efficiency as well as threshing damage rate are significant (*Li et al., 2015*), especially the effect of threshing drum rotational speed on threshing efficiency and threshing damage rate is extremely significant.

RESULTS

Response surface analysis

The response surface analysis of threshing efficiency is shown in Fig. 12. The response surface of threshing clearance and concave clearance on threshing efficiency is shown in Fig. 12a. During the reduction of threshing clearance from 35 mm to 25 mm, the larger the concave clearance, the lower the threshing efficiency; when the concave clearance increased from 9 mm to 11 mm, the threshing efficiency increased with the increase of threshing clearance (*Zhang et al., 2022*). The response surface of threshing drum speed and concave clearance on threshing efficiency is shown in Fig. 12-b. The larger the concave clearance, the lower the threshing efficiency during the decrease of threshing drum speed from 900 r/min to 700 r/min; when the concave clearance increased from 9 mm to 11 mm, the threshing efficiency increased with the increase of threshing drum speed. The response surface of threshing drum speed and threshing clearance on threshing efficiency is shown in Fig.12-c. The larger the threshing clearance, the lower the threshing efficiency when the threshing drum speed decreases from 900 r/min to 700 r/min; when the threshing clearance increases from 25 mm to 35 mm, the threshing efficiency increases with the increase of threshing drum speed.

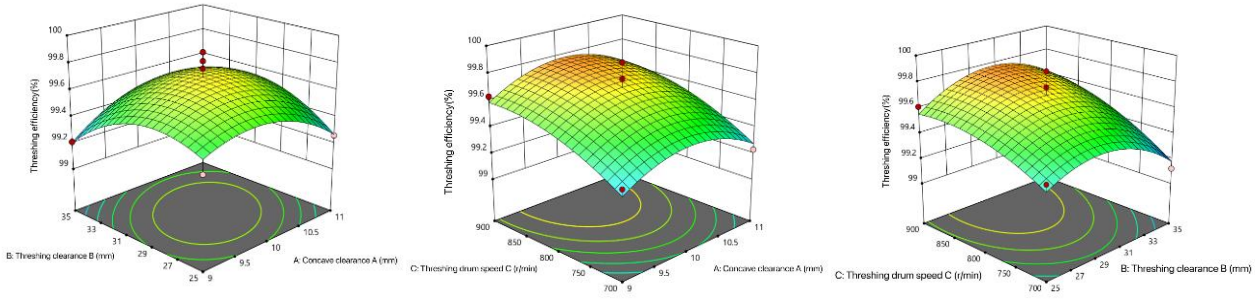

(a) *(b)* *(c)*

Fig. 12 - Response surface analysis of threshing efficiency

The response surface analysis of threshing damage rate is shown in Fig. 13 .The response surface of threshing clearance and concave clearance on threshing damage rate is shown in Fig. 13-a. When the threshing clearance decreases from 13 mm to 11 mm, the larger the concave clearance, the lower the threshing damage rate; when the concave clearance increases from 9 mm to 11 mm, the threshing damage rate decreases with the increase of threshing clearance.

The response surface of threshing drum speed and concave clearance on threshing damage rate is shown in Fig. 13-b. When the threshing drum speed decreased from 900 r/min to 700 r/min, the larger the concave clearance, the lower the threshing damage rate; when the concave clearance increased from 9 mm to 11 mm, the threshing damage rate increased with the increase of threshing drum speed. The response surface of threshing drum speed and threshing clearance on threshing efficiency is shown in Fig. 13-c. When the threshing drum speed decreased from 900 r/min to 700 r/min, the larger the threshing clearance, the lower the threshing damage rate; when the threshing clearance increased from 11 mm to 13 mm, the threshing damage rate increased with the increase of threshing drum speed.

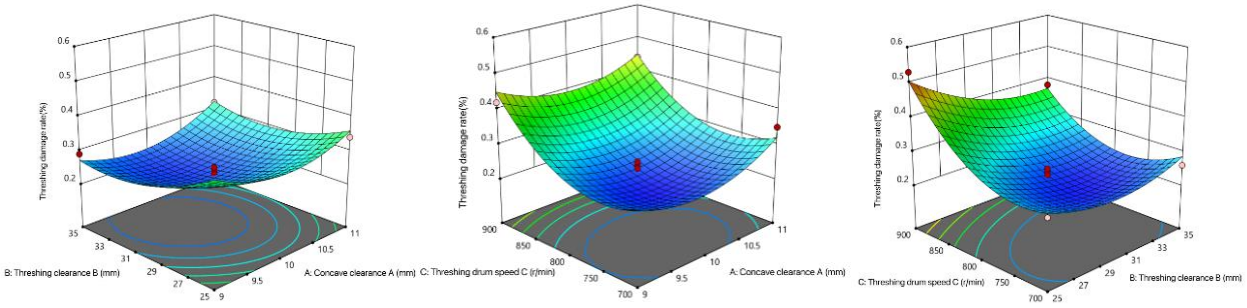

(a) *(b)* *(c)*

Fig. 13 - Response surface analysis of threshing damage rate

The optimal parameters of the threshing drum were determined as follows: speed 800 r/min, concave clearance 10 mm, and threshing clearance 30 mm. After the optimization, the threshing efficiency of the threshing device increased to 98.78% and the damage rate of threshing decreased to 0.62%, which improved the overall performance of the threshing device compared with that before the optimization. It can also be concluded that the parameters affecting the threshing performance in the threshing device include not only the common threshing drum speed (*Wang et al., 2021*), concave clearance, and threshing clearance, but also the size and shape of the threshing elements have a great influence on the detachment effect.

CONCLUSION

(1) The optimized threshing device test bench has the characteristics of high efficiency and low loss. To some extent, it solves the problem of high damage rate of existing threshing devices.

(2) The critical force of grain crushing was determined by mechanical compression test and Herzen contact theorem, and the optimal working parameters were determined by EDEM simulation and optimization: threshing drum speed 800 r/min, concave clearance 10 mm, threshing clearance 30 mm.

(3) The bench test proved that when the rotating speed of the threshing drum was 800 r/min, the gap of the concave plate was 10 mm, the gap of the threshing was 30 mm, and the tilt angle of the test bench was 15 degrees, the corn threshing operation effect was the best. At this time, the threshing efficiency was 98.78%, and the threshing damage rate was 0.62%, which met the requirements of corn threshing operation.

ACKNOWLEDGEMENT

This research was funded by Shandong Province Key R&D Program (Major Science and Technology Innovation Project) Projects and High-performance seeding and harvesting key components and intelligent operation equipment creation (Grant NO.2021CXGC010813). Supported by Postgraduate Innovation Program of Qingdao Agricultural University.

REFERENCES

[1] Bi Quansheng. (2015). *Research on double roller differential speed corn threshing device with tooth spike* [D]. Anhui Agricultural University,

[2] Chen Weilin. (2022). Exploration on the promotion and application of mechanized corn harvesting technology [J]. *Farmers' Counselor*, (16):72-74.

[3] Chen Bingbing, Su Zhanke, Zhang Keping, Hou Chuankai, Sun Bugong, Zhang Peng. (2022). Design and simulation analysis of threshing device of intercropping pea harvester [J]. *Agricultural Equipment and Vehicle Engineering*, 60 (09): 20-25.

[4] China Academy of Agricultural Mechanization Sciences. (2007). *Agricultural Machinery Design Manual (Volume II)* [M]. Beijing: China Agricultural Science and Technology Press.

[5] Di Zhifeng, Cui Zhongkai, Zhang Hua, et al. (2018). Design and experiment of combined riffle block and spike tooth axial flow corn threshing roller [J]. *Journal of Agricultural Engineering*, 34(1): 28-34.
[6] Edvinas Pužauskas, Dainius Steponavičius, Eglė Jotautienė, et al. (2016). Substantiation of concave crossbar shape for corn ear threshing [J]. *Mechanika*, 22(6): 553-561.
[7] Fan C, Cui T, Zhang D, et al. (2019). Design of Feeding Head Spiral Angle Longitudinal Axis Corn Threshing Separation Device Based on EDEM[C]//2019 *ASABE Annual International Meeting. American Society of Agricultural and Biological Engineers*.
[8] Hu B.Y.,Li Y.M. (2018). Finite element simulation analysis of cob collision for corn seed threshing [J]. *Agricultural equipment technology*, 44(04):4-7.
[9] Li X.P., Gao L.X., Ma F.L. et al. (2007). Experiments on the impact damage of corn seeds [J]. *Journal of Shenyang Agricultural University*, (1): 89-93.
[10] Li Junzhong. (2021). *Research and development of key technology and equipment of corn seed direct harvesting based threshing device* [D]. Jilin University. DOI:10.27162/d.cnki.gjlin.2021.004964.
[11] Li X, Du Y, Liu L, et al. (2022). Research on the constitutive model of low-damage corn threshing based on DEM [J]. *Computers and Electronics in Agriculture*, 194: 106722.
[12] Li X, Du Y, Guo J, et al. (2020). Design, simulation, and test of a new threshing cylinder for high moisture content corn [J]. *Applied Sciences*, 10(14): 4925.
[13] Li Jicheng, Guo Lin, Zhang Tianhui. (2015). Analysis of dynamic characteristics of cross flow fan impeller of combine harvester based on fluid structure coupling [J]. *Research on Agricultural Mechanization*, 37 (09): 234-240. DOI: 10.13,427/j.cnki.njyi.2015.09.053.
[14] Qu Zhe. (2018). *Research on low damage combined corn threshing and separating device* [D]. China Agricultural University.
[15] Tang S.H., Jin C.K., Zhang G.H., Guo Hazel, Zhao Nan, Xu Bei. (2022). Research status of threshing and separating device of combine harvester in China [J]. *Agricultural Mechanization Research*, 44(03): 1-9+15. DOI:10.13427/j.cnki.njyi.2022.03.001.
[16] Waree Srison, Somchai Chuan-Udom et al. (2016). Effects of Operating Factors for an Axial-flow Corn Shelling Unit on Losses and Power Consumption [J]. *Agriculture and Natural Resources*, 50(5): 421-425.
[17] Wang Zhanbin, Wang Zhenwei, Zhang Yinping, Wei Xiuting, Liu Chengqiang, Li Lei.(2022). Simulation and experiment of hammer claw type corn threshing device [J]. *Agricultural Mechanization Research*, 44(12):140-147. DOI:10.13427/j.cnki.njyi.2022.12.028.
[18] Wang Meimei, Wang Wanzhang, Yang Liquan, Hou Mingtao. (2018). Research on corn kernel modeling method based on EDEM [J]. *Journal of Henan Agricultural University*, 52 (01): 80-84+103. DOI: 10.16445/j.cnki.1000-2340.2018.01.013.
[19] Wang S, Chen P, Ji J, et al. (2021). Design and experimental study of flexible threshing unit for Chinese cabbage seeds [J]. *INMATEH - Agricultural Engineering*, 65(3), pp.333-344. DOI: https://doi.org/10.35633/inmateh-65-35
[20] Xiao Jinlong, Zhao Jinbao. (2021). Research on virtual prototype of corn straw returning machine based on rigid flexible hybrid modeling [J]. *Agricultural Equipment and Vehicle Engineering*, 59 (05): 47-50.
[21] Yang Yalan, Li Yuliang, Li Ruishu, Chai Shuling, Wei Zhouxia, Hou Qirei. (2022). Thoughts on how to effectively improve the efficiency of corn breeding [J]. *Heilongjiang Grain*, (08): 39-41.
[22] Yan BX, Wu GW, Fu WQ, Gao NNA, Meng ZJ, Zhu P. (2020). Study on the factors influencing the bed position of corn precision seeding with high seed drop based on EDEM [J]. *Journal of Agricultural Machinery*, 51(S2):47-54.
[23] Yu Y, Li L, Zhao J, et al. (2021). Optimal design and simulation analysis of spike tooth threshing component based on DEM [J]. *Processes*, 9(7): 1163.
[24] Zhou Ke-chi, He Chang-an, Ji Chun-xue, Wang Hui, Zhang Heng.(2022). Research on corn breeding problems and countermeasures [J]. Heilongjiang Grain, (04): 64-66.
[25] Zhou Wenjing, Li Wenjuan, Guo Tao, et al. (2022). Effects of species and harvesting time on nutrient composition of silage corn [J]. *Grassland Science*, 39(07):1419-1428.
[26] Zhao Wuyun, Guo Kangquan. (2012). Optimization of working parameters of combined spiral plate tooth seed corn thresher [J]. *Journal of Agricultural Machinery*, 43(12): 56-61.
[27] Zhou Long. (2021). *Simulation analysis and experimental research of corn seed modeling and sowing process based on discrete element method* [D]. Jilin. DOI:10.27162/d.cnki.gjlin.2021.007542.
[28] Zheng Zhaohui. (2020). *Simulation study on seed collision characteristics of corn harvest clearing* [D]. Northeastern Agricultural University. DOI:10.27010/d.cnki.gdbnu.2020.000984.

[29] Zhang T., Li P., Zhang Y., Tang XL, Dai ZG, Li Y. (2021). Analysis of research progress on damage of corn harvesting machinery [J]. *Agricultural Technology and Equipment*, (01): 27-29.
[30] Zhang Xinwei, Yi Kechuan, Gao Lianxing. (2015). Analysis of contact mechanics during the collision between corn seeds and threshing components [J]. *China Agronomy Bulletin*, 31(14): 285-290.
[31] Zhang Longxiang. (2020). *Research and Design of Cleaning Device of Buckwheat Harvester Based on FLUENT-EDEM Coupling* [D]. Chengdu University. DOI: 10.27917/d.cnki.gcxdy.2020.000088.
[32] Zhang Hanzhong, Meng Wenjun, Wang Beibei. (2022). Research on gas-solid two-phase flow field of grab bucket discharge based on CFD-DEM coupling simulation [J]. *Mining Research and Development*, 42 (04): 166-172. DOI: 10.13,827/j.cnki.kyyk.2022.04.011.